# Effect of dipole interaction on collective modes in 3He-A

**L. Tewordt, N. Schopohl, Dieter Vollhardt**

**Angaben zur Veröffentlichung / Publication details:**

Tewordt, L., N. Schopohl, and Dieter Vollhardt. 1977. "Effect of dipole interaction on collective modes in 3He-A." *Journal of Low Temperature Physics* 29 (1-2): 119–47. https://doi.org/10.1007/bf00659092.



# Effect of Dipole Interaction on Collective Modes in $^3$He-A

**L. Tewordt, N. Schopohl, and D. Vollhardt**

*Abteilung für Theoretische Festkörperphysik, Universität Hamburg, Hamburg, Germany*

*A general theory for the correlation functions of superfluid $^3$He which takes into account rigorously the magnetic dipole interaction is developed. The resulting equations are solved for the Anderson–Brinkman–Morel (ABM) state and for wave vectors* **q** *oriented parallel to the energy gap axis. Then the dispersion relations of low-frequency modes, including Fermi liquid corrections and damping due to pair breaking, are calculated in the zero-temperature and zero-field limit. There are two real frequency modes arising from each of the longitudinal and transverse spin density correlation functions: a spin wave and an orbit wave,* both *exhibiting a frequency gap where that of the spin wave is somewhat modified in comparison to the unperturbed longitudinal nuclear magnetic resonance frequency $\Omega_L^{ABM}$. The orbit wave is damped much more strongly than the spin wave. Further, there are two real frequency modes arising from the density correlation function: the sound wave, having a frequency gap of the order $\Omega_L^{ABM}$, and an orbit wave, exhibiting a gap in wave number of order $\Omega_L^{ABM}/v_F$.—The NMR frequency undergoes a small splitting, which is the result of the splitting of the energy gap due to the dipole interaction. One of the two gaps still has nodes.—In addition to these low-frequency modes our equations yield resonances at frequencies of the order of the gap frequency $\Delta_0/\hbar$, i.e., at $\omega = 1.22\ \Delta_0/\hbar$ and at $\omega = 1.58\ \Delta_0/\hbar$. The damping and the oscillator strengths of these resonances are calculated.*

## 1. INTRODUCTION AND DISCUSSION OF RESULTS

The interaction between the magnetic dipoles of the nuclei in superfluid $^3$He is known to determine the equilibrium configuration of the multicomponent order parameter and to give rise to the phenomenon of a *longitudinal* nuclear magnetic resonance (NMR). That the dipole interaction can lead to other important effects was demonstrated first by Tewordt *et al.*[1] (hereafter

referred to as TFDE) and by Tewordt and Einzel.[2] In the infinite-wavelength limit ($q \to 0$) the dipole interaction gives rise to resonances at frequencies $\omega$ of the order of the gap $\Delta$, for instance, at $\omega = (8/5)^{1/2}\Delta$ in the Balian–Werthamer (BW) state and at about $\omega = 2^{1/2}\Delta$ in the Anderson–Brinkman–Morel (ABM) state.[1,4] That the dipole interaction is responsible for these modes can be seen from the fact that the oscillator strengths of these high-frequency resonances go to zero if the dipole interaction goes to zero. Further,[2] in the ABM state the dipole interaction leads to a gap in the wave spectrum of sound waves which is about $\omega \cong (1+F_0^s)^{1/4}\Omega_L^{\mathrm{ABM}}/(1+F_0^a)^{1/2}$. Here $F_0^s$ and $F_0^a$ are Landau parameters and $\Omega_L^{\mathrm{ABM}}$ is the longitudinal NMR frequency.

While the dipole interaction has been considered within the "adiabatic" approximation in the work of Leggett and Takagi,[3] which is closely related to the present work, it has been neglected in most of the other studies of collective modes.[5,7–9] This is understandable since the dipole interaction introduces a coupling of the many (22) degrees of freedom in this system and thus gives rise to extremely complicated equations of motion. In the present paper the dipole interaction will be taken into account rigorously. This is necessary, for instance, in order to determine the oscillator strengths of the high-frequency modes at $q = 0$ (and also for $q \lesssim \Omega_L^{\mathrm{ABM}}/v_F$). The inclusion of the dipole interaction is also the only way to see which of the low-frequency modes are the true Goldstone-boson modes ($q \to 0$, $\omega \to 0$), which are associated with the broken *overall* rotational symmetry and with the broken gauge symmetry. We shall see that none of the real frequency modes found in this calculation are true Goldstone modes, because the dipole interaction gives rise either to a frequency gap or to a wave number gap in the dispersion curves of these modes. Therefore we have to conclude that the Goldstone modes must have imaginary or complex frequencies. In the present work we have calculated only the real frequency modes.

First we generalize the equations of TFDE[1] for the correlation functions, which have been derived in the presence of the dipole interaction, to include states having an anisotropic energy gap like that of the ABM state (the equations of TFDE are strictly valid only for the BW state) and, further, to include finite wave vectors $\mathbf{q}$. Then we specialize these equations to the ABM state and to orientations of $\mathbf{q}$ parallel to the equilibrium axis $\boldsymbol{l}$ of the energy gap. This is because we are interested in analytic results and the 18 linear equations describing the order parameter fluctuations can only be solved analytically for $\mathbf{q} \| \boldsymbol{l}$. Explicit expressions for the various susceptibilities, frequency gaps, and damping terms, and figures for the dispersion curves will be given only for the zero-temperature limit, where some analytic results can be obtained. From these exact results we can see clearly how the collective modes in $^3$He-A should be classified and what their physical meaning is.

In calculating the collective modes by this method it is essential to stay within the framework of the self-consistent random phase approximation, which means in the first place that the nine equations for the nine equilibrium order parameter components have to be solved self-consistently in the presence of the dipole interaction. Starting from the Leggett configuration of the ABM state,[6] which minimizes the dipole energy, it is found that this state is slightly modified such that it is no longer unitary.[2] This has the consequence that the pair average spin is no longer zero. We shall calculate the two quasiparticle energies corresponding to quasiparticle spin along or against the direction of the pair average spin.[6] The interesting result is that one of the two energy gaps (which differ by terms of the order of the dipole shift) still has nodes along $\boldsymbol{l}$. It turns out that this splitting of the energy gap leads to a splitting of the NMR frequency (and all the other frequency gaps) which is of the order of a few tenths of a percent. Thus it is unlikely that this splitting can be observed. The reason for this splitting is that the dynamical properties depend sensitively on the detailed structure of the energy gap for $\mathbf{k}$ in the vicinity of $\boldsymbol{l}$.

For $\mathbf{q} \| \boldsymbol{l}$ the 18 linear equations for the 18 components of the order parameter fluctuations are found to decouple into two sets of five and two sets of four equations. The order parameter fluctuations involved in the two sets of five equations couple to the longitudinal and transverse spin density fluctuations, respectively. We consider the limiting case where the magnetic field (pointing along the $z$ direction while $\boldsymbol{l}$ is in the $y$ direction) goes to zero. Since the direction of the field is implicitly given by our representation of the order parameter, we still can speak of longitudinal and transverse polarization. Then, in the zero-field limit, the dispersion relations for the collective modes arising from the solutions of these two sets of five equations become the same. We find two real frequency modes arising from each of the longitudinal and transverse spin density correlation functions (see Fig. 3):

(a) The spin wave dispersion curve (lower curve in Fig. 3) tends to $\omega = (1+F_0^a)^{1/2} v_F q/\sqrt{3}$ for large $q$, and $\omega$ goes to a finite value at $q=0$, which is somewhat below the original NMR frequency $\Omega_L^{\mathrm{ABM}}$. This is an effect due to the coupling to the orbit wave. The corresponding order parameter deviations from equilibrium are shown in Fig. 2a. These deviations are represented in terms of deviations of the vectors $\mathbf{d}$, $\mathbf{m}$, $\mathbf{n}$, and $\boldsymbol{l}$ from equilibrium, where $\mathbf{d}$ determines the spin axes and where $\mathbf{n}$, $\mathbf{m}$, and $\boldsymbol{l} = \mathbf{m} \times \mathbf{n}$ determine the orbital axes of the Cooper-pair wave function. The frequency gap is due to oscillations of the vector $\mathbf{d}$ about $\boldsymbol{l}$ and the fact that the dipole interaction is proportional to $-(\mathbf{d} \cdot \boldsymbol{l})^2$. The corresponding dispersion curve of the original order parameter mode that induces this spin density mode is shown in Fig. 1 (lower solid curve).

(b) The dispersion of the orbit wave (upper curve in Fig. 3) tends approximately to $\omega = v_F q$ for large $q$, and $\omega$ again goes to a finite value of the

order $\Omega_L^{\mathrm{ABM}}$ as $q$ tends to zero. The deviations of the order parameter components from equilibrium for this mode are shown in Fig. 2b. Now the $\boldsymbol{l}$ vector oscillates about the fixed $\mathbf{d}$ vector, thus producing a frequency gap. The dispersion curve of the original order parameter mode that induces this spin density mode is shown in Fig. 1 (upper solid curve). The damping of this orbit wave is several orders of magnitude larger than that of the spin wave in (a).

It is satisfying that our equation determining the wave spectra of the order parameter modes coupling to spin density (Fig. 1) can be written in a form which is quite similar to that of the phenomenological theory of Leggett and Takagi[3] describing the resonance between the orbital mode and the NMR mode. However, our expression for the "Cooper-pair orbital susceptibility" $\chi_{\mathrm{orb}}$ and the "normal locking energy constant" $g_n$ describing the inertia and the depth of the potential well for the oscillations of $\boldsymbol{l}$ are generalized to include the $\omega$ and $q$ dependence and also the imaginary parts arising from pair breaking and Landau damping processes. In particular, at $q=0$ and $T=0$ we find that $\chi_{\mathrm{orb}} \sim N(0) \ln (T_c/\omega)$ and that $\omega\tau$ and $\omega\tau_{\mathrm{K}}$ are both of the order $\ln (T_c/\omega)$. Here $\tau$ and $\tau_{\mathrm{K}}$ are the two relaxation times which have been introduced phenomenologically in Ref. 3 to describe the damping of the orbital motion, and $\omega$ is the frequency gap of the orbit wave, which is of the order of the dipole shift.

Next we consider those order parameter fluctuations that couple to the density fluctuations. These are given by the solutions of one set of four equations, while the solutions of the other set of four equations vanish identically. We find two real frequency modes arising from the density correlation function (see Fig. 6):

(c) For the lower dispersion curve in Fig. 6 the frequency $\omega$ tends approximately to $v_{\mathrm{F}}q$ for large $q$, and $\omega$ goes to zero as $q$ tends from above to a certain finite value $q_0$, being of the order $\Omega_L^{\mathrm{ABM}}/v_{\mathrm{F}}$. For $q<q_0$ this solution disappears, and therefore this mode has a true gap with respect to wave number.

(d) The upper dispersion curve in Fig. 6 tends to $\omega=(1+F_0^s)^{1/2}v_{\mathrm{F}}q/\sqrt{3}$ for large $q$ (sound wave dispersion), and $\omega$ becomes finite and of the order $\Omega_L^{\mathrm{ABM}}$ at $q=0$.

The dispersion curves of the original order parameter modes that induce the density modes of Fig. 6 are shown in Fig. 4. The deviations of the order parameter components from equilibrium that are involved in the Anderson–Bogoliubov phonon mode[10,11] (see lower solid curve in Fig. 4) are shown in Fig. 5a. One sees that the vectors $\mathbf{d}$, $\mathbf{n}$, and $\mathbf{m}$ maintain their equilibrium directions but oscillate in magnitude. The deviations of the order parameter components from equilibrium that are involved in the orbit wave (upper solid curve in Fig. 4) are shown in Fig. 5b. It should be pointed

out that the order parameter modes corresponding to Figs. 5a and 5b by themselves would not lead to a frequency gap or a wave number gap, because the vectors **d** and **l** do not move apart from each other. The corresponding dispersion curves are the dashed curves in Fig. 4. However, these modes are coupled via the dipole interaction and this gives rise to the frequency and wave number gaps in the solid curves in Figs. 4 and 6.

The coupling of the Anderson–Bogoliubov phonon mode (Fig. 4, lower solid curve) to the density changes the asymptotic behavior for large $q$ from $\omega = v_F q/\sqrt{3}$ to $\omega = (1+F_0^s)^{1/2} v_F q/\sqrt{3}$. Since the Fermi liquid parameter $F_0^s$ is very large ($F_0^s \simeq 90$, see Ref. 12), the latter dispersion curve would intersect that of the orbit wave (upper solid curve in Fig. 4). This gives rise to hybridization between the sound wave and the orbit wave, the effect being that the sound wave acquires a frequency gap and the orbit wave acquires a wave number gap.

In addition to the low-frequency resonances ($\omega \sim \Omega_L^{ABM}$), the equations determining the poles of the spin density, density, and order parameter correlation functions yield high-frequency resonances ($\omega \sim \Delta$). At $T = 0$ and $q = 0$ the latter become equal to $1.50\Delta$ and $1.93\Delta$ for the spin density correlation functions, and there is only one resonance at $1.93\Delta$ of the density correlation function.[4] The damping of these modes is given explicitly by our results for the imaginary parts of the susceptibilities, which are valid for all frequencies (see Appendix B). From these results we estimate that $\omega\tau \sim 1$. In Ref. 1 only approximate values for the high-frequency resonances were obtained, since the anisotropy of the gap was neglected. These estimates gave values of $2\Delta^{1/2}$ and $2\Delta$, which have to be compared with the correct values, i.e., $1.50\Delta$ and $1.93\Delta$. The modes at $1.50\Delta = 1.22\Delta_0$ and $1.93\Delta = 1.58\Delta_0$ are nothing else than Wölfle's "clapping" and "superflapping" modes.[5] Here $\Delta_0$ is the amplitude of the gap parameter in the ABM state and $\Delta$ is the average value of the gap [they are connected by the relation $\Delta_0 = (3/2)^{1/2}\Delta$]. The "clapping" and "flapping" motions of the vectors **m** and **n** are shown in Figs. 2a and 2b, respectively. For $q = 0$, and more generally for $\mathbf{q} \| \mathbf{l}$, the oscillator strengths of these modes are found to be smaller by a factor of order $(\Omega_L^{ABM}/\Delta)^2$ than those of the low-frequency modes.

At first sight the results of this paper seem to be of purely academic interest because some of the new effects shown to be caused by the dipole interaction become important only at temperatures where the normal locking energy is smaller than the dipole energy, that is, for $T \lesssim 10^{-2} T_c$. Here we note that our calculation refers only to zero temperature and zero magnetic field. From the phenomenological theory of Leggett and Takagi[3] one can infer, however, that the resonance between the transverse NMR mode and the orbital mode (see the two curves in Fig. 3) can be shifted into

an experimentally accessible temperature range by means of a finite magnetic field. Thus, for comparison with experiment it is desirable to generalize the present theory to include a magnetic field and to work out the general expressions given in this paper for finite temperatures. It would be also interesting to see what happens to the coupling effects between the sound wave and the orbit wave (see Fig. 6) when the temperature increases.

In Section 2 the general theory of the random phase correlation functions is developed, valid for anisotropic energy gaps, finite wave vectors $\mathbf{q}$, all frequencies, and all temperatures. In Section 3 this theory is specialized to the ABM state and to $\mathbf{q} \| \boldsymbol{l}$. Wave spectra of low-frequency modes and high-frequency resonances are calculated explicitly at $T = 0$.

## 2. GENERAL THEORY

In Eqs. (33)–(35) and Fig. 1 of Ref. 1 general equations have been presented which describe the coupling between the spin fluctuations (four-point function $T$) and the order parameter fluctuations (four-point functions $T'$ and $T''$). The four-point interaction function $\Gamma$ contains the spin-exchange interaction of strength $I$, the BCS pairing interaction of strength $g$, and the dipole interaction of strength $\gamma^2$. Inserting into these equations the expansions of the functions $\Gamma$, $T$, $T'$, and $T''$ with respect to spin and orbital space, one finds 22 coupled linear equations for the four components of $T$, $t_{\nu\mu}$ ($\nu = 0, 1, 2, 3$, and $\mu$ fixed), and the 18 components of $T'$ and $T''$, $t'^{i}_{\nu\mu}$ and $t''^{i}_{\nu\mu}$ ($\nu = 0, 1, 3$, and $i = x, y, z$, and $\mu$ fixed). The subscripts $\nu$ and $\mu$ refer to the Pauli matrices $\tau^{\nu}$ (including the unit matrix for $\nu = 0$), and the superscripts $i$ refer to the components with respect to the direction cosine $\hat{k}_i$ of the momentum $\mathbf{k}$. Since the subscript $\mu$ is fixed and the same for all the components, it can be considered as a dummy variable in the following equations. The physical meaning of the components $t_{\nu\mu}$ is that $t_{00}$ describes the density oscillations while the components $t_{11}$, $t_{22}$, and $t_{33}$ describe the spin fluctuations. The components $t'^{i}_{\nu\mu}$ correspond to small deviations of the order parameter components from their equilibrium values $d_{i\lambda}$, and the components $t''^{i}_{\nu\mu}$ are the conjugate complex of the $t'^{i}_{\nu\mu}$. Note, however, that $t'^{i}_{0\mu}$ is the deviation of $d_{i2}$, $t'^{i}_{1\mu}$ is the deviation of $d_{i3}$, and $t'^{i}_{3\mu}$ gives the deviation of $d_{i1}$ since the gap matrix is defined by $\hat{\Delta} = \hat{k}_i d_{i\lambda} \tau^{\lambda} i\tau^2$.

In Ref. 1 the dependence of the square of the energy gap, $|\Delta(\hat{k})|^2$ on $\hat{k}$ was neglected, and further, the wave number $\mathbf{q}$ of the modes was taken to be zero. In this paper we present the generalized equations needed to deal with the ABM state and finite $\mathbf{q}$. The coefficients of the first set of equations [see Eq. (51), Ref. 1], i.e.,

$$a^{ij}_{\nu\eta} t'^{j}_{\eta\mu} - k^{ij}_{\nu\eta} t''^{j}_{\eta\mu} = A^{i}_{\nu\mu} \tag{1}$$

have to be modified as follows:

$$a^{ij}_{\nu\eta} = \delta_{\nu\eta}\delta_{ij} + V^{iil}_{\nu\eta}\bar{\chi}_{lj} \tag{2}$$

$$k^{ij}_{\nu\eta} = V^{iip}_{\nu\gamma} d_{m\lambda} d_{n\kappa} \tfrac{1}{2} \mathrm{Tr}\,(\tau^{\gamma}\tau^{\lambda}\tau^{2}\tau^{\eta}\tau^{\kappa}\tau^{2}) K^{nj}_{pm} \tag{3}$$

$$A^{i}_{\nu\mu} = \tfrac{2}{3} V^{iij}_{\nu\gamma} W_{jl} d_{l\eta} \tfrac{1}{2} \mathrm{Tr}\,(\tau^{\gamma}\tau^{\delta}\tau^{\eta} i\tau^{2}) t_{\delta\mu} \tag{4}$$

Here the $V^{iil}_{\nu\eta}$ are the potentials, either proportional to $g$ or to $\gamma^2$ [see Eq. (47), Ref. 1], and

$$\bar{\chi}_{lj}(\mathbf{q}, i\omega_m) = N(0)T \sum_{\omega_n} \int d\varepsilon_k \int \frac{d\Omega}{4\pi} \hat{k}_l \hat{k}_j \frac{(i\omega_n + \varepsilon_k)(i\omega_{m-n} + \varepsilon_{k-q})}{(\omega_n^2 + E_k^2)(\omega_{m-n}^2 + E_{k-q}^2)} \tag{5}$$

$$K^{nj}_{pm}(\mathbf{q}, i\omega_m) = N(0)T \sum_{\omega_n} \int d\varepsilon_k \int \frac{d\Omega}{4\pi} \frac{\hat{k}_p \hat{k}_m \hat{k}_n \hat{k}_j}{(\omega_n^2 + E_k^2)(\omega_{m-n}^2 + E_{k-q}^2)} \tag{6}$$

$$W_{jl}(\mathbf{q}, i\omega_m) = 3N(0)T \sum_{\omega_n} \int d\varepsilon_k \int \frac{d\Omega}{4\pi} \hat{k}_j \hat{k}_l \frac{i\omega_n + \varepsilon_k}{(\omega_n^2 + E_k^2)(\omega_{m-n}^2 + E_{k-q}^2)} \tag{7}$$

Further, $E_k^2 = \varepsilon_k^2 + |\Delta(\hat{k})|^2$, and $\Omega$ is the solid angle in the direction of $\hat{k}$. Neglecting the $\hat{k}$ dependence of the energy gap and going to the limit $\mathbf{q} \to 0$, one recovers the expressions in Eqs. (56)–(58) of TFDE.[1]

The second set of equations is obtained from Eq. (1) by taking the complex conjugate of this equation and making use of the relation $t^{\nu i}_{\nu\mu} = (t^{ii}_{\nu\mu})^*$. Instead of these two sets of equations, one can also use Eqs. (60) and (61) of TFDE[1] for Re $t^{ii}_{\nu\mu}$ and Im $t^{ii}_{\nu\mu}$.

The third set of equations describing the coupling between the spin fluctuation components $t_{\nu\mu}$ and the order parameter fluctuations $t^{ii}_{\nu\mu}$ is given by

$$t_{\nu\mu} = \tfrac{1}{2} V_{\nu\nu}\delta_{\nu\mu} + V_{\nu\nu}(\chi_{GG}\delta_{\nu\eta} + \chi^{\nu\eta}_{FF}) t_{\eta\mu} + E_{\nu\mu} + H_{\nu\mu} \tag{8}$$

where according to the spin-fluctuation model, $V_{11} = V_{22} = V_{33} = -V_{00} = (1/2)I$. The susceptibilities for the particle–hole channel occurring in Eq. (8) are defined in terms of the Green's functions $G$, $F$, and $\bar{F}$ as follows:

$$\chi_{GG}(\mathbf{q}, i\omega_m) = -2N(0)T \sum_{\omega_n} \int d\varepsilon_k \int \frac{d\Omega}{4\pi} G(\mathbf{k}, i\omega_n) G(\mathbf{k}+\mathbf{q}, i\omega_{n+m}) \tag{9}$$

$$\chi^{\nu\mu}_{FF}(\mathbf{q}, i\omega_m) = 2N(0)T \sum_{\omega_n} \int d\varepsilon_k \int \frac{d\Omega}{4\pi}$$

$$\times \frac{1}{2} \mathrm{Tr}\,[\tau^{\nu tr} \bar{F}(\mathbf{k}+\mathbf{q}, i\omega_{m+n}) \tau^{\mu} F(\mathbf{k}, i\omega_n)] \tag{10}$$

The coupling terms in Eq. (8) are equal to

$$E_{\nu\mu} = (H_{\nu\mu})^* = \tfrac{2}{3} V_{\nu\nu} W_{ij} d^*_{i\eta} t'^{ij}_{\gamma\mu} \tfrac{1}{2} \mathrm{Tr}\,(\tau^\nu \tau^\gamma \tau^2 i\tau^\eta) \tag{11}$$

The diagonal coefficients $a^{ii}_{\nu\nu}$ can be simplified by making use of the gap equation. For this it is essential to stay in the framework of the self-consistent approximation for the random phase correlation function, that is, the Hartree–Fock approximation for the self-energy. Including the dipole interaction, the latter leads to the following nine equations for the order parameter components $d_{ij}$ (see Ref. 2):

$$-d_{ix}\delta_{\nu 3} + id_{iy}\delta_{\nu 0} + d_{iz}\delta_{\nu 1} = -V'^{in}_{\nu\mu}(-d_{jx}\delta_{\mu 3} + id_{jy}\delta_{\mu 0} + d_{jz}\delta_{\mu 1})(\bar{\chi}_0)_{nj} \tag{12}$$

Here

$$(\bar{\chi}_0)_{ij} = N(0) T \sum_{\omega_n} \int d\varepsilon_k \int \frac{d\Omega}{4\pi} \frac{\hat{k}_i \hat{k}_j}{\omega_n^2 + E_k^2} \tag{13}$$

Neglecting the $\hat{k}$ dependence of the energy gap, one recovers Eqs. (62) and (63) of TDFE.[1]

## 3. COLLECTIVE MODES IN THE ABM STATE

For the ABM state we take the representation where $d_{xy} = -id_{zy} = (3/2)^{1/2}\Delta \equiv \Delta_0$. It has been shown in Ref. 2 that self-consistency of Eq. (12) can be achieved only by allowing $d_{yx}$ and $d_{yz}$ to be different from zero. The gap equation becomes then

$$1 = -[g - (12/5)\pi\gamma^2](\bar{\chi}_0)_{xx} \tag{14}$$

For zero temperature one finds that $d_{yx}/d_{xy} = d_{yz}/d_{zy} = 3\mu$, where $\mu = 36\pi\gamma^2/5N(0)g^2 \sim 10^{-6}$ is a measure of the dipole coupling strength. This state is no longer unitary. The eigenvalues of $\hat{\Delta}\hat{\Delta}^\dagger$ are given by

$$|\Delta(\hat{k})|^2 = \Delta_0^2[(\hat{k}_x^2 + \hat{k}_z^2 + \bar{\mu}^2\hat{k}_y^2)^{1/2} \pm \bar{\mu}|\hat{k}_y|]^2 \tag{15}$$

Here the $\hat{k}_i$ are the direction cosines of the wave vector $\mathbf{k}$ and $\bar{\mu} = 3\mu$. According to Leggett,[6] these eigenvalues correspond to the energy gaps for quasiparticle spin along or against the direction of the "pair average spin." It is interesting to notice that the energy gap corresponding to the lower sign still has nodes along the equilibrium direction of the order parameter axis $\boldsymbol{l}$ (in our representation given by $|\hat{k}_y| = 1$, $\hat{k}_x = \hat{k}_z = 0$).

We consider now the 18 linear equations for the order parameter fluctuations Re $t'^{ij}_{\eta\mu}$ and Im $t'^{ij}_{\eta\mu}$ [see Eqs. (60) and (61) of TFDE[1]], which arise from Eq. (1) and its complex conjugate. The coefficients occurring in these equations are defined in Eqs. (2)–(7). In eliminating the term 1 in the

diagonal components $a^{ii}_{\nu\nu}$ [see Eq. (2)], it is essential to use the self-consistent gap equation (14). While we consider in this paper the dipole interaction contributions to the coefficients $a^{ij}_{\nu\eta}$ arising from the potentials $V'^{il}_{\nu\eta}$ [see Eq. (47) of TFDE[1]], we neglect these contributions in the coefficients $k^{ij}_{\nu\eta}$. This means that we neglect strong coupling corrections of order $N(0)g$ [actually, of order $10^{-1}N(0)g$] in comparison to one.

The resulting 18 linear equations for the order parameter fluctuations $\mathrm{Re}\, t'^{ij}_{\eta\mu}$ and $\mathrm{Im}\, t'^{ij}_{\eta\mu}$ are found to decouple into two sets of five and two sets of four equations if the wave vector $\mathbf{q}$ is parallel to $\boldsymbol{l}$ (here along the $y$ axis). In this paper we shall treat only this special case. To save space, we shall not write down these equations explicitly but discuss the solutions separately.

### 3.1. Order Parameter Modes Coupling to Spin Fluctuations

The two sets of five equations involve the order parameter fluctuations $\mathrm{Re}\, t'^{lx}_{1\mu}$, $\mathrm{Im}\, t'^{lx}_{3\mu}$, $\mathrm{Re}\, t'^{lz}_{3\mu}$, $\mathrm{Im}\, t'^{lz}_{1\mu}$, $\mathrm{Re}\, t'^{ly}_{0\mu}$, and $\mathrm{Im}\, t'^{lx}_{1\mu}$, $\mathrm{Re}\, t'^{lx}_{3\mu}$ $\mathrm{Im}\, t'^{lz}_{3\mu}$, $\mathrm{Re}'^{lz}_{1\mu}$, $\mathrm{Im}\, t'^{ly}_{0\mu}$, respectively. The first set of fluctuations couples to the spin fluctuation component $t_{33}$, and the second set couples to $t_{11}$. The denominators of both sets of solutions are identical. Setting this denominator equal to zero, we obtain the following equation for the poles with respect to frequency $\omega$ at given wave number $\mathbf{q}$:

$$\mathrm{Det} \equiv \left(a_x - 3\mu - \frac{2\mu^2}{a_y - 2\mu}\right)(a_x^2 - \mu^2) - 4b^2\left(a_x - \mu - \frac{\mu^2}{a_y - 2\mu}\right) = 0 \quad (16)$$

The terms $a_x$ and $a_y$ arise from the diagonal coefficients $a^{ii}_{\nu\nu}$ in Eq. (2) [divided by $(1/2)N(0)g$] by making use of the gap equation (14):

$$a_x \equiv 2[N(0)]^{-1}[\bar{\chi}_{xx} - (\bar{\chi}_0)_{xx}] \quad (17)$$

$$a_y \equiv 2[N(0)]^{-1}\{[\bar{\chi}_{yy} - (\bar{\chi}_0)_{yy}] - [(\bar{\chi}_0)_{xx} - (\bar{\chi}_0)_{yy}]\} \quad (18)$$

The quantities $\mu = 36\pi\gamma^2/5N(0)g^2$ are due to the dipole interaction contributions to the coefficients $a^{ij}_{\nu\eta}$ arising from the potentials $V'^{il}_{\nu\eta}$ in Eq. (2) [see Eq. (47) of TFDE[1]]. The term $b$ arises from the coefficients $k^{ij}_{\nu\eta}$ in Eq. (3) and thus from the quantities $K^{nj}_{pm}$ defined in Eq. (6) [again divided by $(1/2)N(0)g$]:

$$b \equiv 3[N(0)]^{-1}\Delta^2(K^{xx}_{zz} - K^{zx}_{xz}) = 6[N(0)]^{-1}\Delta^2 K^{zz}_{xx} \quad (19)$$

Carrying out the frequency sums over $\omega_n$ [see Eqs. (5) and (6)], we find that

all quantities $a_x$, $a_y$, and $b$ can be expressed in terms of a single function $F$:

$$a_x = \int \frac{d\Omega}{4\pi} \hat{k}_x^2 [\omega^2 - v_F^2(\hat{\mathbf{k}} \cdot \mathbf{q})^2 - 2|\Delta(\hat{k})|^2] F \tag{20}$$

$$a_y = \int \frac{d\Omega}{4\pi} \hat{k}_y^2 \{[\omega^2 - v_F^2(\hat{\mathbf{k}} \cdot \mathbf{q})^2] F - 2|\Delta(\hat{k})|^2 \left[ F + \int_0^\infty \frac{d\varepsilon_k}{2E_k^3} \left( \frac{E_k}{2T} \cosh^{-2} \frac{E_k}{2T} - \tanh \frac{E_k}{2T} \right) \right] \} \tag{21}$$

$$b = \int \frac{d\Omega}{4\pi} \hat{k}_x^2 |\Delta(\hat{k})|^2 F \tag{22}$$

where $d\Omega$ is the solid angle in the direction of $\hat{k}$. The function $F$ is equal to

$$F(\hat{k}; \mathbf{q}, \omega) = \int_{-\infty}^{+\infty} d\varepsilon_k \frac{1}{[(\omega + i\delta)^2 - (E_k + E_{k-q})^2][(\omega + i\delta)^2 - (E_k - E_{k-q})^2]} \times \left\{ \frac{E_{k-q}^2 - E_k^2 - \omega^2}{2E_k} \tanh \frac{E_k}{2T} + \frac{E_k^2 - E_{k-q}^2 - \omega^2}{2E_{k-q}} \tanh \frac{E_{k-q}}{2T} \right\} \tag{23}$$

The function $F$ and its angle averages occurring in Eqs. (20)–(22) are treated in Appendix A for the zero-temperature limit. The integral over $\varepsilon_k$ in Eq. (23) is carried out analytically, but for the remaining integrals over $x \equiv \cos\theta = \hat{k}_y$ we have to restrict ourselves to numerical computation.

It is interesting that Eq. (16) can be rewritten in a form which is similar to that of the phenomenological theory of Leggett and Takagi[3] describing the resonance between the orbital mode and the NMR mode. To see this, we denote the expressions multiplying $\omega^2$ in Eqs. (20) and (21) for $a_x$ and $a_y$ by $\chi_{\text{spin}}/N(0)\Delta^2$ and $\chi_{\text{orb}}/N(0)\Delta^2$, respectively, and we denote the second term in Eq. (21) involving $|\Delta(\hat{k})|^2$ by $-g_n/N(0)\Delta^2$. In fact, in the limit $\mathbf{q} \to 0$ and $\omega \to 0$ these quantities essentially reduce to the corresponding quantities in Ref. 3. The physical meaning of $\chi_{\text{spin}}$ and $\chi_{\text{orb}}$ as transverse and longitudinal susceptibilities with respect to $\boldsymbol{l}$ is obvious because these terms arise from $\bar{\chi}_{xx} - (\bar{\chi}_0)_x$ and $\bar{\chi}_{yy} - (\bar{\chi}_0)_y$ [see Eqs. (17) and (18)]. However, the "normal locking term" $g_n$ originates in our microscopic theory from making use of the correct gap equation (14), which leads to a term proportional to $(\bar{\chi}_0)_x - (\bar{\chi}_0)_y$ [see second term in Eq. (18)]. Since the gap equation corresponds to the minimum of the energy of the system, $g_n$ is indeed a measure of the energy change as $\boldsymbol{l}$ is rotated at fixed quasiparticle occupation.[7,8]

Expanding Eq. (16) up to and including terms of order $\mu^2$, we obtain the equation

$$(a_x + 2b - \mu)(a_y - 2\mu) = \tfrac{1}{2}\mu^2 \tag{24}$$

Expressing in Eq. (24) the quantities $a_x + 2b$ and $a_y$ in terms of the quantities $\chi_{\text{spin}}$, $\chi_{\text{orb}}$, and $g_n$ as defined above, we obtain

$$\left[\omega^2 - \langle v_F^2(\hat{\mathbf{k}}\cdot\mathbf{q})^2\rangle_x - \frac{\mu N(0)\Delta^2}{\chi_{\text{spin}}}\right]\left[\omega^2 - \langle v_F^2(\hat{\mathbf{k}}\cdot\mathbf{q})^2\rangle_y - \frac{g_n}{\chi_{\text{orb}}} - 2\frac{\mu N(0)\Delta^2}{\chi_{\text{orb}}}\right]$$
$$= \frac{1}{2}\mu^2\frac{[N(0)\Delta^2]^2}{\chi_{\text{spin}}\chi_{\text{orb}}} \tag{25}$$

Here the brackets $\langle\ \rangle_i$ denote averages over the solid angle of $\hat{k}$, where the weighting function is equal to $\hat{k}_i^2 F$. In comparison to Eq. (9) of Ref. 3, our Eq. (25) is specialized to zero field, but it is generalized to finite $\mathbf{q}\|\boldsymbol{l}$.

In our theory the coupling of the NMR mode and the orbital mode is given explicitly by the relation $t'^y_{0\mu} = -i\mu(t'^x_{3\mu} - t'^z_{1\mu})/(a_y - 2\mu)$. Indeed, $t'^y_{0\mu}$ is an "orbital" fluctuation component, giving rise to oscillations of the order parameter axis $\boldsymbol{l}$ about its equilibrium position, while the other fluctuation components $t'^x_{1\mu}$, $t'^x_{3\mu}$, $t'^z_{1\mu}$, and $t'^z_{3\mu}$ do not change the direction of $\boldsymbol{l}$. This can be seen from the fact that for $|\hat{k}_y| = 1$, $\hat{k}_x = \hat{k}_z = 0$, only the deviations $t'^y_{\nu\mu}$ of the order parameter components from their equilibrium values can make the energy gap different from zero.

We have calculated numerically all dispersion relations arising from Eq. (16) in the zero-temperature limit with the help of Eqs. (20)–(22) for $a_x$, $a_y$, and $b$, by inserting into the integrands the expression for $F$ as given in Eqs. (A4), (A13), and (A18), and then numerically carrying out the integrations over $x \equiv \cos\theta = \hat{k}_y$. The results are shown in Fig. 1 (solid curves), where $\omega/\mu^{1/2}\Delta_0$ is plotted vs. $qv_F/\mu^{1/2}\Delta_0$. One sees that both modes exhibit gaps at $q = 0$, one at $\omega_1 \cong 2\mu^{1/2}\Delta_0$ and the other at $\omega_2 \cong 0.7\mu^{1/2}\Delta_0$. With the help of Eqs. (25), (30), and (31), we find the following approximate expressions for these frequency gaps:

$$\left(\frac{\omega_1}{2\mu^{1/2}\Delta_0}\right)^2 \cong 1 + (2\ln\mu^{-1})^{-1}; \qquad \left(\frac{\omega_2}{2\mu^{1/2}\Delta_0}\right)^2 \cong 3(2\ln\mu^{-1})^{-1} \tag{26}$$

For large $q$, $\omega$ tends approximately to $v_F q$ (orbit wave[3,5,9]) and to $v_F q/\sqrt{3}$ (spin wave), respectively. More exactly, the values of $\omega$ of the orbit wave for $qv_F/\mu^{1/2}\Delta_0 \gg 1$ are given by Eq. (46). It is obvious from Fig. 1 that both modes are strongly coupled with each other. To see this more clearly, we have plotted also the wave spectra of the uncoupled spin and orbit waves arising from the equation $a_x + 2b = \mu$ (spin wave, see dashed curve in Fig. 1 tending to the straight line of slope $1/\sqrt{3}$) and from the equation $a_y = 2\mu$ (orbit wave, see dashed curve in Fig. 1 tending approximately to a straight line of slope 1).

The quantities $a_x + 2b$ and $a_y$ and thus the dispersion relation in Eq. (16) are determined mainly by the susceptibilities $\chi_{\text{spin}}$ and $\chi_{\text{orb}}$ and by the

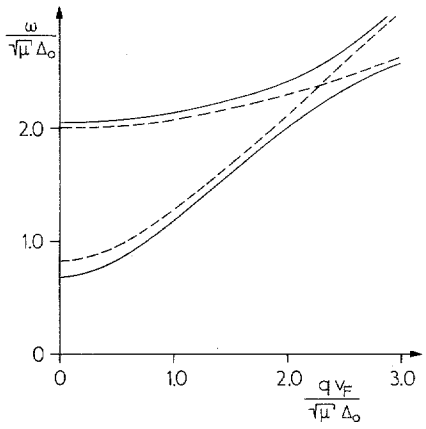


Fig. 1. Dispersion curves of order parameter modes coupling to spin density. We use reduced frequencies $\omega/\mu^{1/2}\Delta_0$ and reduced wave numbers $qv_F/\mu^{1/2}\Delta_0$, where $\Delta_0$ is the gap parameter, $\mu$ ($=10^{-6}$) is the dipole interaction strength, and $v_F$ is the Fermi velocity. The upper curve is the orbit wave and the lower curve is the spin wave. Dashed curves hold in the absence of the dipole coupling.

normal locking term $g_n$. From the definitions given above for these quantities we obtain with the help of Eqs. (20), (21), and (A4) the following integrals over $x = \cos\theta = \hat{k}_y$:

$$\frac{\chi_{\text{spin}}}{N(0)} \equiv \Delta^2 \int \frac{d\Omega}{4\pi} \hat{k}_x^2 F(\hat{k}; \mathbf{q}, \omega) = \frac{1}{6}\int_{-1}^{+1} dx\,(1-x^2)\tilde{F}(x; \tilde{q}, \tilde{\omega}) \tag{27}$$

$$\frac{\chi_{\text{orb}}}{N(0)} \equiv \Delta^2 \int \frac{d\Omega}{4\pi} \hat{k}_y^2 F(\hat{k}; \mathbf{q}, \omega) = \frac{1}{3}\int_{-1}^{+1} dx\, x^2 \tilde{F}(x; \tilde{q}, \tilde{\omega}) \tag{28}$$

where $\tilde{\omega} \equiv \omega/\Delta_0$ and $\tilde{q} \equiv qv_F/\Delta_0$, and at $T = 0$ the normal locking term becomes equal to [see Eq. (21), second term]

$$\frac{g_n}{N(0)\Delta^2} = \int_{-1}^{+1} dx\, x^2(1-x^2)\left\{\tilde{F}(x; \tilde{q}, \tilde{\omega}) - \frac{1}{2}\frac{1}{1-x^2}\right\} \tag{29}$$

In the limit $q \to 0$ we have obtained analytic expressions for the different $x$ integrals over Re $\tilde{F}$ and Im $\tilde{F}$ occurring in Eqs. (27)–(29). The results are given in Appendix B. With the help of these results we find, to leading order with respect to expansions in terms of the small quantity $\omega/\Delta_0$,

$$\begin{aligned}
&\text{Re}\,\frac{\chi_{\text{spin}}}{N(0)} \cong \frac{1}{6}; && \text{Im}\,\frac{\chi_{\text{spin}}}{N(0)} \cong \frac{\pi}{72}\left(\frac{\omega}{\Delta_0}\right)^2 \\
&\text{Re}\,\frac{\chi_{\text{orb}}}{N(0)} \cong \frac{1}{6}\ln\left[16\left(\frac{\Delta_0}{\omega}\right)^2\right]; && \text{Im}\,\frac{\chi_{\text{orb}}}{N(0)} \cong \frac{\pi}{12} \\
&\text{Re}\,\frac{g_n}{N(0)\Delta^2} \cong \frac{3}{64}\left(\frac{\omega}{\Delta_0}\right)^2 \ln\left[16\left(\frac{\Delta_0}{\omega}\right)^2\right]; && \text{Im}\,\frac{g_n}{N(0)\Delta^2} \cong \frac{\pi}{12}\left(\frac{\omega}{\Delta_0}\right)^2
\end{aligned} \tag{30}$$

It is interesting to see from Eq. (30) that $\chi_{\text{orb}}$ is much larger than $\chi_{\text{spin}}$:

Re $\chi_{\text{orb}}$ even diverges for $\omega \to 0$, and Im $[\chi_{\text{orb}}/N(0)] \sim 1$. This result is clearly due to the nodes of the energy gap, as can be seen from Eqs. (27) and (28) and the fact that $\tilde{F}$ as a function of $x = \hat{k}_y$ diverges as $x$ tends to one. It should be pointed out that the expressions for the frequency gaps $\omega_1$ and $\omega_2$ in Eq. (26) have been calculated from Eqs. (25) and (30) by neglecting all imaginary parts and also Re $g_n$. The latter approximation means that we have neglected in Eq. (25) the term $g_n/\chi_{\text{orb}} \cong (3/16)\omega^2$ in comparison to the term $\omega^2$.

Comparing Eqs. (25) and (30) with Eq. (8) of Ref. 3, we find that the phenomenological relaxation times $\tau_K$ and $\tau$ introduced in Ref. 3 to describe the damping of the orbital motion are given by

$$\omega\tau_K = \frac{\operatorname{Re}\chi_{\text{orb}}}{\operatorname{Im}\chi_{\text{orb}}} \cong \frac{2}{\pi} \ln\left[16\left(\frac{\Delta_0}{\omega}\right)^2\right]$$
$$\omega\tau = \frac{\operatorname{Re} g_n}{\operatorname{Im} g_n} \cong \frac{9}{16\pi} \ln\left[16\left(\frac{\Delta_0}{\omega}\right)^2\right] \tag{31}$$

Responsible for these damping terms is the pair-breaking mechanism [see the denominator in the expression for $F$, Eq. (23)], which takes place in the vicinity of the nodes of the energy gap where the gap is smaller than $\omega$. For $\omega = \omega_1$ or $\omega = \omega_2$ the values of $\omega\tau_K$ and $\omega\tau$ are about 10 and 3, respectively.

A physical explanation of the properties of the different order parameter modes derived above can be obtained by considering the nature of the deviations of the order parameter from equilibrium that are generated, for instance, by the set of components Re $t_{1\mu}^{lx}$, Im $t_{3\mu}^{lx}$, Re $t_{3\mu}^{lz}$, Im $t_{1\mu}^{lz}$, and Re $t_{0\mu}^{ly}$. For an interpretation of these components we write the order parameter components in the form $d_{j\lambda} = \Delta_0(n_j + im_j)d_\lambda$, where $n_j$ and $m_j$ are the components of the vectors $\mathbf{n}$ and $\mathbf{m}$ determining the orbital axes and where $d_\lambda$ are the components of the vector $\mathbf{d}$ determining the spin axes. The vector $\boldsymbol{l}$ is given by $\boldsymbol{l} = \mathbf{m} \times \mathbf{n}$. For equilibrium we have in our representation $\mathbf{n} = \hat{x}$, $\mathbf{m} = \hat{z}$, and $\mathbf{d} = \hat{y}$. Then one sees from the definition of the $t_{\eta\mu}^{lj}$ that Im $t_{3\mu}^{lx}$ generates a deviation of the vector $\mathbf{m}$ lying in the $xz$ plane, and simultaneously it generates a deviation of the vector $\mathbf{d}$ lying in the $xy$ plane (see Fig. 2a). Further, the component Re $t_{3\mu}^{lz}$ generates a deviation of $\mathbf{n}$ lying in the $xz$ plane, and simultaneously it leads to a deviation of $\mathbf{d}$ lying in the $xy$ plane (see Fig. 2a). The direction of $\boldsymbol{l} = \mathbf{m} \times \mathbf{n}$ stays fixed along the $y$ axis for both components Im $t_{3\mu}^{lx}$ and Re $t_{3\mu}^{lz}$, while the vector $\mathbf{d}$ moves in the $xy$ plane. Therefore, since the dipole interaction is proportional to $-(\mathbf{d} \cdot \boldsymbol{l})^2$, this leads to a gap of the order of the dipole shift in the wave spectrum of the corresponding mode, provided that $\mathbf{n}$ and $\mathbf{m}$ move in phase ($\mathbf{n} \cdot \mathbf{m} = 0$). If $\mathbf{n}$ and $\mathbf{m}$ move in counterphase, one has the "clapping mode" whose frequency is of the order of $\Delta_0$. This mode is also a solution of Eq. (16) and it will be

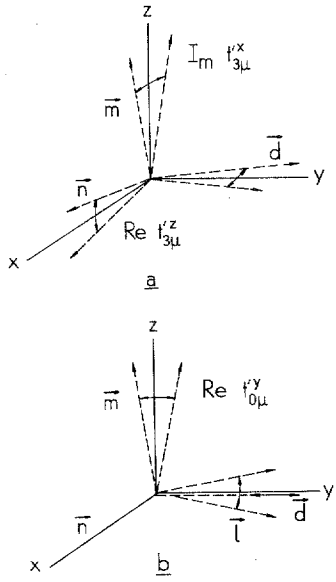


Fig. 2. Deviations of vectors **d**, **n**, **m**, and $\boldsymbol{l} = \mathbf{m} \times \mathbf{n}$ from equilibrium (where **d** determines the spin axes and **n**, **m**, and $\boldsymbol{l}$ determine the orbital axes of the Cooper-pair wave function), for order parameter fluctuations corresponding to (a) spin wave and (b) orbit wave coupling to spin density.

discussed below. As we shall see later, the components Im $t'^{x}_{3\mu}$ and Re $t'^{z}_{3\mu}$ couple to the spin fluctuation component $t_{33}$.

We consider now the orbital component Re $t'^{y}_{0\mu}$. This generates a deviation of **m** lying in the $yz$ plane, and simultaneously it generates an oscillation of **d** in the direction of the $y$ axis (see Fig. 2b). Since $\boldsymbol{l} = \mathbf{m} \times \mathbf{n}$ moves away from the $y$ axis and thus from the direction of **d**, this mode again acquires a gap. The strong coupling of these modes for small **q** which is evident from Fig. 1, originates in the relation Re $t'^{y}_{0\mu} = \mu(\mathrm{Im}\, t'^{x}_{3\mu} - \mathrm{Im}\, t'^{z}_{1\mu})/(a_y - 2\mu)$ between the orbital and the spin components. Here the remaining components in our set of five fluctuation components, i.e., Re $t'^{x}_{1\mu}$ and Im $t'^{z}_{1\mu}$, are smaller by a factor $\mu$ than the three components discussed above and therefore they can be neglected in this context.

The results for the wave spectra of the order parameter modes shown in Fig. 1 have been calculated by using the zeroth order energy gap, $|\Delta(\hat{k})|^2 = \Delta_0^2(\hat{k}_x^2 + \hat{k}_z^2) = \Delta_0^2(1 - x^2)$. We have also calculated these wave spectra by using the two self-consistent energy gaps given in Eq. (15) or Eqs. (A2) and (A3). The result is that the effect of the correction terms of order $\mu$ on the wave spectra is negligible, because the splittings of both frequency gaps $\omega_1$ and $\omega_2$ turn out to be about 0.2% for $\mu = 10^{-6}$.

We consider now the coupling of these modes of the order parameter to the spin fluctuations. It turns out that for the ABM state only the coupling terms $E_{\nu\nu} + H_{\nu\nu}$ for $\nu = 1$ and 3 occurring in the equations for the spin

fluctuation components $t_{11}$ and $t_{33}$ [see Eq. (8)] become different from zero. In the latter the components $\mathrm{Re}\, t_{3\mu}^{tz}$ and $\mathrm{Im}\, t_{3\mu}^{tx}$ enter. Inserting these solutions into Eq. (11), we find the following expressions for the "fluctuation" susceptibility $\chi_{tl}^{33}$:

$$\chi_{tl}^{33} \equiv \frac{E_{33}+H_{33}}{V_{33}t_{33}} = -\frac{8}{3}[N(0)]^{-1}\Delta^2 W_{xx}^2\,\mathrm{Det}^{-1} \times\left\{\left(a_x - 2\mu - \frac{\mu^2}{a_y-2\mu}\right)(a_x+\mu) + \left(a_x - 3\mu - \frac{2\mu^2}{a_y-2\mu}\right)a_x - 4b\left(a_x - \mu - \frac{\mu^2}{a_y-2\mu}\right)\right\} \tag{32}$$

Here the expression for Det is given in Eq. (16). The term $W_{xx}$ is defined in Eq. (7); it can be expressed in terms of the function $F$:

$$W_{xx}(\mathbf{q},\omega) = \frac{3}{2}N(0)\omega\int\frac{d\Omega}{4\pi}\hat{k}_x^2 F(\hat{k};\mathbf{q},\omega) \tag{33}$$

According to Eqs. (8) and (32), the poles of $t_{33}$ are given by the equation

$$1 - \tfrac{1}{2}I(\chi_{GG} + \chi_{FF}^{33} + \chi_{tl}^{33}) = 0 \tag{34}$$

Here we have set $V_{33} = (1/2)I$, where $I$ is the spin fluctuation model parameter. The fluctuation susceptibility $\chi_{tl}^{33}$ is defined in Eq. (32). The susceptibility $\chi_{FF}^{33}$ arising from two anomalous propagators in the particle–hole channel is defined in Eq. (10). Again it can be expressed in terms of the function $F$ defined by Eq. (23):

$$\chi_{FF}^{33}(\mathbf{q},\omega) = \chi_{FF}^{00}(\mathbf{q},\omega) = 2N(0)\int\frac{d\Omega}{4\pi}|\Delta(\hat{k})|^2 F(\hat{k};\mathbf{q},\omega) \tag{35}$$

Most crucial in Eq. (34) is the particle–hole susceptibility $\chi_{GG}$ defined by Eq. (9), which reduces in the limit $\Delta_0 \to 0$ to the Lindhard function $\chi_n$. The evaluation of $\chi_{GG}$ is rather involved. For the zero-temperature limit it is carried out in Appendix C. For the real part we obtain [see Eq. (C3)]

$$\mathrm{Re}\,\chi_{GG}(\mathbf{q},\omega) = \mathrm{Re}\,\chi_n + 2N(0) \times\int\frac{d\Omega}{4\pi}\frac{\omega^2 + v_F^2(\hat{\mathbf{k}}\cdot\mathbf{q})^2}{\omega^2 - v_F^2(\hat{\mathbf{k}}\cdot\mathbf{q})^2}|\Delta(\hat{k})|^2 F(\hat{k};\mathbf{q},\omega) \tag{36}$$

We have calculated numerically from Eq. (34) with the help of Eqs. (16), (32), (33), (35), and (36) all dispersion relations in the zero-temperature limit. The results are shown in Fig. 3 for a spin fluctuation parameter $\bar{I} \equiv N(0)I$, which is taken to be equal to the Landau parameter

$-F_0^a \cong 0.75$. The two resulting wave spectra having finite frequency gaps at $q = 0$ are induced by the term $\chi_{ll}^{33}$ in Eq. (34) and thus by the modes of the order parameter whose dispersion relations are shown in Fig. 1 (solid curves). The new frequency gaps occurring in Fig. 3 are modified in comparison to the frequency gaps $\omega_1$ and $\omega_2$ of the order parameter modes [see Eq. (26)] by the quantity $(1-\bar{I})$. This can be seen from our approximate analytic expressions for these frequency gaps, which have been derived from Eq. (34) with the help of Eq. (30) and the fact that for $\omega > 0$, $q \to 0$, $\mathrm{Re}\,\chi_{\bar{F}\bar{F}} \cong N(0)$ and $\mathrm{Re}\,\chi_{GG} \cong N(0)$ [see Eqs. (35) and (36)]. Then we find that the new frequency gaps are given by the solutions of the following two equations corresponding to the two signs:

$$(\omega/2\mu^{1/2}\Delta_0)^2 = \tfrac{1}{2}(1-\bar{I}) + [\ln(16\Delta_0^2\omega^{-2})]^{-1} \pm \tfrac{1}{2}(\{(1-\bar{I}) - [\ln(16\Delta_0^2\omega^{-2})]^{-1}\}^2 + 3[\ln(16\Delta_0^2\omega^{-2})]^{-2})^2 \quad (37)$$

It should be noticed that the ordinary longitudinal NMR frequency, $\Omega_L^{\mathrm{ABM}}$, is

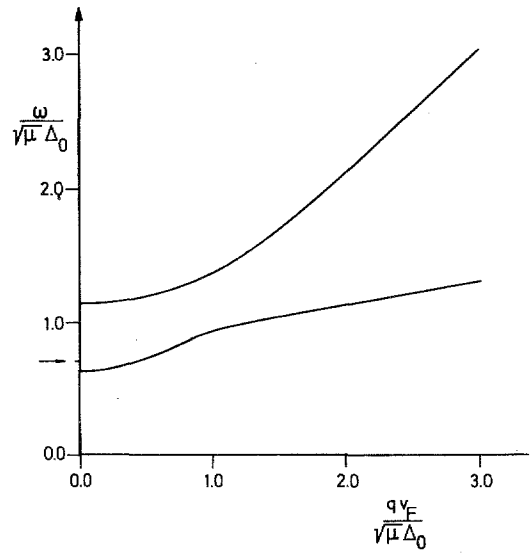


Fig. 3. Dispersion curves of low-frequency modes arising from spin density correlation functions, in reduced units (see Fig. 1), for a spin fluctuation parameter $\bar{I} = -F_0^a = 0.75$. Upper curve: orbit wave. Lower curve: spin wave. The arrow indicates the unperturbed longitudinal NMR frequency $\Omega_L^{\mathrm{ABM}}$, which is given by $\Omega_L^{\mathrm{ABM}}/\mu^{1/2}\Delta_0 = 2^{1/2}(1-\bar{I})^{1/2}$.

given by[1] $\Omega_L^{ABM}/\mu^{1/2}\Delta_0 = [2(1-\bar{I})]^{1/2} \cong 0.71$ for $\bar{I} = -F_0^a = 0.75$. Thus the ratio of the actual NMR frequency (see gap in Fig. 3) to $\Omega_L^{ABM}$ (see arrow in Fig. 3) becomes $0.61/0.71 \cong 0.86$. This effect is apparently due to the coupling between the spin wave and the orbit wave.

It should be emphasized that the poles of the order parameter fluctuation components Re $t_{1\mu}^{lx}$, Im $t_{3\mu}^{lx}$, Re $t_{3\mu}^{lz}$, Im $t_{1\mu}^{lz}$, and Re $t_{0\mu}^{ly}$ are in reality not given by Eq. (16), that is, Det = 0, but by Eq. (34), and therefore these poles are identical to those of $t_{33}$. This is because our solutions for these order parameter fluctuation components contain the term $t_{33}/\mathrm{Det}$ as a factor. The poles of the other five order parameter fluctuation components that couple to the spin density component $t_{11}$ are found to be the same as those of $t_{33}$.

The coupling between the spin wave and the orbit wave becomes vanishingly small as the temperature increases once the normal locking part of $a_y$ becomes much larger than the dipole term $\mu$. According to our estimate of $g_n$, this occurs for $T/T_c \gg 10^{-2}$. The reason for the smallness of the coupling is that for $a_y \gg \mu$ the terms $\mu^2/(a_y - 2\mu)$ in Eq. (16) become much smaller than $\mu$. Under these conditions the zeros of Eq. (16) are given to a good approximation by the equations $a_x + 2b = \mu$ (spin wave) and $a_y = 2\mu$ ("normal flapping mode"[5]).

In addition to these low-frequency resonances ($\omega \sim \mu^{1/2}\Delta$), Eqs. (16) and (34) yield high-frequency resonances ($\omega \sim \Delta$). To zeroth order in $\gamma^2$ or $\mu$ we obtain these high-frequency resonances from Eq. (32) for the fluctuation susceptibility $\chi_{ll}^{33}$ by multiplying this expression by $(a_y - 2\mu)$ and then going to the limit $\mu \to 0$. The denominator of the resulting expression becomes equal to $a_x a_y (a_x - 2b)(a_x + 2b)$. The equation $a_x - 2b = 0$ has no solution. The equation $a_x + 2b = 0$ has for $q \to 0$ the solution $\omega \to 0$, which goes over into the longitudinal NMR frequency if $\mu$ becomes finite. Finally, we have to consider the following two equations:

$$a_x = 0 \tag{38}$$

$$a_y = 0 \tag{39}$$

In the zero-temperature limit and for $q \to 0$ we obtain analytic expressions for $a_x$ and $a_y$ by inserting into Eqs. (20) and (21) the corresponding $x$ integrals over $x^{2m}\tilde{F}(x; \tilde{q}, \tilde{\omega})$ given in Appendix B. Then the following solutions of Eqs. (38) and (39) are found[4]:

$$\omega = 1.50\Delta = 1.22\Delta_0 \quad \text{[from Eq. (38)]} \tag{40}$$

$$\omega = 1.93\Delta = 1.58\Delta_0 \quad \text{[from Eq, (39)]} \tag{41}$$

Here $\Delta_0 \equiv (3/2)^{1/2}\Delta$ is the amplitude of the ABM gap parameter. For the damping $1/\tau$ of these modes we find with the help of the results of Appendix

B that $\omega\tau \sim 1$. In Ref. 1 resonances were found at $\omega = 2^{1/2}\Delta$ and at $\omega \lesssim 2\Delta$ by using an angular average of the ABM gap and neglecting $\omega$ occurring in the function $F$ in Eq. (23). One sees that these estimates are rather close to the accurate values given in Eqs. (40) and (41). The numerical value of $1.22\Delta_0$ is identical to that obtained by Wölfle[5] in the absence of dipole forces for his "clapping mode," and the value $1.58\Delta_0$ is close to the value $(12/5)^{1/2}\Delta_0$ for his "super-flapping mode."

However, in the absence of the dipole interaction and for $\mathbf{q} \| \boldsymbol{l}$ these high-frequency modes do not couple to the spin fluctuations. This can be seen from the coupling term $E_{33}+H_{33}$ in Eq. (32): Multiplying this expression by $a_y - 2\mu$ and going to the limit $\mu \to 0$ leads to a numerator which contains $a_x$ and $a_y$ as factors. This means that the residues for the poles given by Eqs. (40) and (41) vanish. Therefore it is necessary to go to the next higher order in $\mu$. This has the effect that the residues of $t_{33}$ at these new resonance frequencies become finite and of order $\mu^2$.

### 3.2. Order Parameter Fluctuations Coupling to Density Fluctuations

The two sets of four equations for the order parameter fluctuations involve the components Im $t^{lx}_{0\mu}$, Re $t^{lz}_{0\mu}$, Im $t^{ly}_{1\mu}$, Re $t^{ly}_{3\mu}$, and Re $t^{lx}_{0\mu}$, Im $t^{lz}_{0\mu}$, Re $t^{ly}_{1\mu}$, Im $t^{ly}_{3\mu}$, respectively. The solutions of the second set of equations are identically zero, and the solutions of the first set are given by

$$\begin{aligned}
\operatorname{Im} t^{lx}_{00} &= \tfrac{4}{3}[N(0)]^{-1}\Delta_0 W_{xx}(\mathrm{Det}')^{-1}(a_y+\mu^2)t_{00} \\
\operatorname{Re} t^{lz}_{00} &= -\tfrac{4}{3}[N(0)]^{-1}\Delta_0 W_{xx}(\mathrm{Det}')^{-1}(a_y+\mu^2)t_{00} \\
\operatorname{Im} t^{ly}_{10} &= \tfrac{4}{3}[N(0)]^{-1}\Delta_0 W_{xx}(\mathrm{Det}')^{-1}\mu(1+a_x+2b)t_{00} \\
\operatorname{Re} t^{ly}_{30} &= -\tfrac{4}{3}[N(0)]^{-1}\Delta_0 W_{xx}(\mathrm{Det}')^{-1}\mu(1+a_x+2b)t_{00}
\end{aligned} \tag{42}$$

The poles of these solutions are given by setting the denominator determinant, Det', equal to zero. This yields the equation

$$\mathrm{Det}' \equiv (a_x+2b)a_y - \mu^2 = 0 \tag{43}$$

The quantities $a_x$, $a_y$, and $b$ are defined in Eqs. (20)–(22).

The order parameter fluctuation components given by Eqs. (42) couple to the density fluctuation component $t_{00}$. The coupling term $E_{00}+H_{00}$ [see Eq. (11)] occurring in the equation for $t_{00}$ [see Eq. (8)] is determined by Im $t^{lx}_{00}$ and Re $t^{lz}_{00}$. The explicit expression for the corresponding "fluctuation" susceptibility $\chi^{00}_{tl}$ is given by

$$\chi^{00}_{tl} \equiv \frac{E_{00}+H_{00}}{V_{00}t_{00}} = -\frac{16}{3}[N(0)]^{-1}\Delta^2 W^2_{xx}\frac{a_y+\mu^2}{(a_x+2b)a_y-\mu^2} \tag{44}$$

The relations between the "orbital" fluctuation components in this set of solutions [see Eq. (42)] that change the direction of $\boldsymbol{l}$ and those that leave $\boldsymbol{l}$ unchanged are approximately given by $\operatorname{Im} t_{10}^{\prime y} \cong -\mu \operatorname{Re} t_{00}^{\prime z}/a_y$ and $\operatorname{Re} t_{30}^{\prime y} \cong -\mu \operatorname{Im} t_{00}^{\prime x}/a_y$.

In the zero-temperature limit we obtain numerically from Eq. (43) with the help of the expressions for $a_x$, $a_y$, and $b$ in Eqs. (20)–(22) and $F$ as given in Eq. (A13) or (A18) the two wave spectra as shown in Fig. 4 (solid curves). Again we have plotted $\omega/\mu^{1/2}\Delta_0$ vs. $v_F q/\mu^{1/2}\Delta_0$. One sees that one mode exhibits a frequency gap at $q = 0$, being of the order of the dipole shift, $\omega_3 \sim \mu^{1/2}\Delta_0$. Our approximate analytic expression, which is obtained from Eq. (43) with the help of Eq. (30), becomes

$$(\omega_3/2\mu^{1/2}\Delta_0)^2 \cong (\ln \mu^{-1})^{-1/2} \tag{45}$$

For $q v_F/\mu^{1/2}\Delta_0 \gg 1$, $\omega$ tends approximately to $v_F q$. Analytically we find

$$\omega \to v_F q\{1 + [6 \ln (v_F^2 q^2/4\Delta_0^2)]^{-1}\}^{1/2} \tag{46}$$

The second mode shown in Fig. 4 exhibits a gap with respect to wave number $q$ which is of the order $q_0 \sim \mu^{1/2}\Delta_0/v_F$, and $\omega$ tends asymptotically to $v_F q/\sqrt{3}$ for large $q$. For comparison we have plotted also in Fig. 4 the wave spectra of these modes in the absence of the dipole interaction, which are given by the equation $a_y = 0$ [dashed curve having a slope of about 1 for large $q$, more exactly, Eq. (46)], and by the equation $a_x + 2b = 0$ (dashed straight line of slope $1/\sqrt{3}$).

A physical explanation of the properties of these modes can be achieved again by considering the nature of the deviations of the order parameter components from their equilibrium values, which are generated by the components of this set of equations [see Eq. (42)]. The component $\operatorname{Re} t_{0\mu}^{\prime z}$

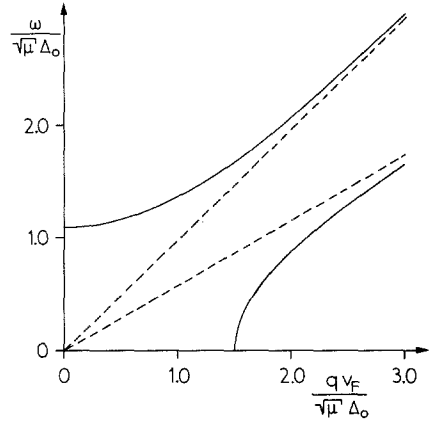


Fig. 4. Wave spectra of order parameter modes coupling to density, in reduced units (see Fig. 1). Upper two curves: orbit wave. Lower two curves: Anderson–Bogoliubov phonon mode. Dashed curves hold for vanishing dipole interaction.

generates an oscillation in magnitude of **m** in the direction of the $z$ axis, and simultaneously it leads to an oscillation in magnitude of **d** along the $y$ axis (see Fig. 5a). And Im $t'^{x}_{0\mu}$ generates a similar oscillation of **n** in the direction of the $x$ axis, and simultaneously it leads to an oscillation of **d** in the direction of the $y$ axis. Thus we see that these two components, Re $t'^{z}_{0\mu}$ and Im $t'^{x}_{0\mu}$, which are coupled to the density fluctuation component $t_{00}$ (see the discussion given above) must give rise to a mode having no frequency gap at $q = 0$. This mode corresponds to the dashed straight line of slope $1/\sqrt{3}$ in Fig. 4.

Next we consider the components Re $t'^{y}_{3\mu}$ and Im $t'^{y}_{1\mu}$. The first component generates a deviation of **n** lying in the $xy$ plane, and simultaneously it gives rise to a deviation of **d** lying in the $xy$ plane (see Fig. 5b). The component Im $t'^{y}_{1\mu}$ leads to a deviation of **m** lying in the $yz$ plane, and simultaneously it generates a deviation of **d** lying in the $yz$ plane (see Fig. 5b). But since Re $t'^{y}_{3\mu} = -\text{Im}\, t'^{y}_{1\mu}$, one always has $\mathbf{n} \cdot \mathbf{m} = 0$, which means that the distorted order parameter stays within the ABM manifold of states. Further, the vector $\boldsymbol{l} = \mathbf{m} \times \mathbf{n}$ and the vector **d** maintain the same directions and therefore these two components themselves would not lead to a frequency gap. The resulting mode corresponds to the upper dashed curve in Fig. 4.

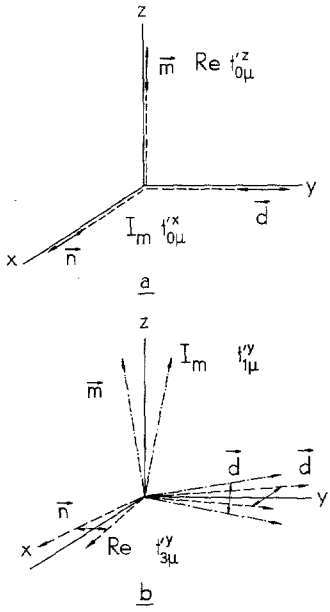


Fig. 5. Deviations of spin axis vector **d** and orbital axis vectors **n** and **m** from equilibrium for order parameter fluctuations corresponding to (a) Anderson–Bogoliubov phonon mode and (b) orbit wave coupling to density.

However, in the presence of the dipole interaction the two modes discussed above are coupled via the relations $\mathrm{Re}\, t_{30}^{ty} = -\mu\, \mathrm{Im}\, t_{00}^{tx}/a_y$ and $\mathrm{Im}\, t_{10}^{ty} = -\mu\, \mathrm{Re}\, t_{00}^{tz}/a_y$. Since $\mu/a_y$ becomes of order 1 if $\omega/\mu^{1/2}\Delta_0$ and $v_F q/\mu^{1/2}\Delta_0$ are of order 1, one can understand why these modes acquire a frequency gap and a wave number gap, respectively (see Fig. 4, solid curves).

According to Eqs. (8) and (44), the poles of the density fluctuation component $t_{00}$ are given by the equation

$$1 + \tfrac{1}{2}F_0^s[N(0)]^{-1}(\chi_{GG} + \chi_{\vec{F}\vec{F}}^{00} + \chi_{tt}^{00}) = 0 \tag{47}$$

Here we have set $V_{00} = -F_0^s/2N(0)$ such that Eq. (47) reduces for the normal phase to the equation determining the dispersions of sound waves in terms of the Landau parameter $F_0^s$. We have calculated numerically from Eq. (47) with the help of Eqs. (33), (35), (36), (44), and Appendix A all dispersion relations in the zero-temperature limit. The results are shown in Fig. 6 for a Landau parameter $F_0^s = 90$ (see Ref. 12). The dispersion curve exhibiting a finite frequency gap and the dispersion curve having a finite wave number gap correspond to the two dispersion curves of the order parameter modes coupling to density that are shown in Fig. 4 (solid curves).

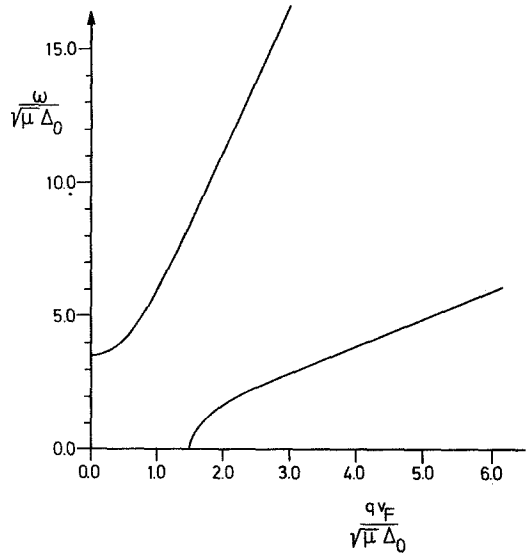


Fig. 6. Wave spectra of low-frequency modes arising from density correlation function, in reduced units (See Fig. 1), for a Landau parameter $F_0^s = 90$. Upper curve: sound wave. Lower curve: orbit wave.

The frequency gap of the upper curve in Fig. 6 is modified by the quantity $(1+F_0^s)^{1/4}$ in comparison to the frequency gap $\omega_3$ of the orbit wave given by Eq. (45). Analytically we find from Eq. (47) together with Eqs. (33), (35), (36), and (44), by taking the limit $q \to 0$ ($\omega > 0$) and using Eq. (30), the following equation for this frequency gap:

$$(\omega/2\mu^{1/2}\Delta_0)^2 \cong (1+F_0^s)^{1/2}[\ln(16\Delta_0^2\omega^{-2})]^{-1/2} \tag{48}$$

This result for the sound wave gap, apart from the factor of order $[\ln \mu^{-1}]^{-1/2} \sim 1$ on the right-hand side of Eq. (48), has been derived already in Ref. 2 [see Eq. (9) in Ref. 2, where $(1+\bar{I})^{1/2}$ in the numerator corresponds to $(1+F_0^s)^{1/2}$ in Eq. (48), and where $(\Omega_L^{\mathrm{ABM}})^2 = 2(\mu^{1/2}\Delta_0)^2(1-\bar{I})$]. The asymptotic behavior of the upper curve in Fig. 6 for large $q$ is that of the sound wave, i.e., $\omega = (1+F_0^s)^{1/2} v_F q/\sqrt{3}$.

The wave number gap of the lower curve in Fig. 6 corresponds to that of the lower curve in Fig. 4 (the Anderson–Bogoliubov phonon mode) while the asymptotic behavior of the lower curve in Fig. 6 for large $q$, i.e., $\omega \cong v_F q$, corresponds to that of the upper curve in Fig. 4 (the orbit wave). Apparently the dispersion curves of Fig. 6 arise from those of Fig. 4 by hybridization between the sound wave and the orbit wave because, due to the large value of the Fermi liquid parameter $F_0^s$ (~90, see Ref. 12), the sound wave dispersion curve would intersect the orbit wave dispersion curve.

It should be pointed out that in reality the poles of the order parameter fluctuation components are not given by Eq. (43), that is, $\mathrm{Det}' = 0$, but by Eq. (47), and thus these poles are identical to the poles of $t_{00}$. This can be seen from Eq. (42) because all solutions of the order parameter fluctuation components contain $t_{00}/\mathrm{Det}'$ as a factor.

In addition to these low-frequency modes ($\omega \sim \mu^{1/2}\Delta$), we again find a high-frequency mode ($\omega \sim \Delta$) from Eqs. (43) and (47). To zeroth order in $\mu$, this is obtained from the expression for the coupling term $E_{00}+H_{00}$ in Eq. (44) by going to the limit $\mu \to 0$. Then the denominator becomes equal to $(a_x+2b)a_y$. For $q=0$ the equation $a_x+2b=0$ has only a zero at $\omega=0$. But the equation $a_y=0$ [see Eq. (39)] yields the solution for the super-flapping mode given by Eq. (41) for $q=0$ and $T=0$. Of course, the residue of this resonance frequency is zero. For finite $\mu$, however, the pole of $\chi_{fl}^{00}$ and thus of $t_{00}$ is shifted from the value given in Eq. (41) by an amount of order $\mu$ and this has the effect that the residue becomes finite and of order $\mu^2$. This vanishing of the strength of the coupling between the super-flapping mode and the sound wave for $\mathbf{q} \| \boldsymbol{l}$ in the absence of the dipole interaction is in agreement with the result of Ref. 5. Finally, Eq. (44) shows that there exists no clapping mode at all [see Eqs. (38) and (40)] for this set of order parameter fluctuations if $\mathbf{q} \| \boldsymbol{l}$. The damping of these modes can be calculated easily with the help of Eqs. (B11)–(B13).

## APPENDIX A. INVESTIGATION OF THE FUNCTION $F$

The function $F(\hat{k}; \mathbf{q}, \omega)$, which arises basically from the integration and summation over the product of two anomalous Green's functions, is of major importance. This is so because all the quantities $a_x$, $a_y$, $b$, $W_{xx}$, $\chi_{GG}$, and $\chi_{\bar{F}F}$ considered in this paper [see Eqs. (20)–(22) and (34)–(36)] can be expressed in terms of $F$. This function is obtained from the analytical continuation to real frequencies ($i\omega_m \to \omega + i\delta$) of the following function:

$$F(\hat{k}; \mathbf{q}, i\omega_m) = T \sum_{\omega_n} \int d\varepsilon_k \frac{1}{(\omega_n^2 + E_k^2)(\omega_{m-n}^2 + E_{k-q}^2)} \tag{A1}$$

where $\omega_n = (2n+1)\pi T$ and $E_k^2 = \varepsilon_k^2 + |\Delta(\hat{k})|^2$. After carrying out the summation and after analytical continuation we obtain the expression for $F$ as given in Eq. (23).

We now concentrate on $T = 0$. Further, we specialize to directions of $\mathbf{q}$ along the nodes of the energy gap, that is, in our representation [see Eq. (15)], $\mathbf{q}$ along the $y$ axis. We choose polar coordinates $\theta$ and $\phi$ in such a way that the polar axis is in the direction of the $y$ axis. Thus the direction cosines of the momentum $\mathbf{k}$ become $\hat{k}_x = (1-x^2)^{1/2} \cos\phi$, $\hat{k}_z = (1-x^2)^{1/2} \sin\phi$, $\hat{k}_y = x$, where $x = \cos\theta$. Then the energy gaps in Eq. (15) become equal to

$$|\Delta(\hat{k})|^2 = \Delta_0^2 \rho_x^2 \tag{A2}$$

where

$$\rho_x^2 = [(1 - x^2 + \bar{\mu}^2 x^2)^{1/2} \pm \bar{\mu}|x|]^2 \tag{A3}$$

The expression for $F$ in Eq. (23) can now be transformed into

$$F(\hat{k}; \mathbf{q}, \omega) = (1/\Delta_0^2) \tilde{F}(x; \tilde{q}, \tilde{\omega}) \tag{A4}$$

where $\tilde{q}$ and $\tilde{\omega}$ are reduced variables, i.e.,

$$\tilde{q} \equiv v_F q/\Delta_0, \qquad \tilde{\omega} \equiv \omega/\Delta_0 \tag{A5}$$

and where $\tilde{F}$ is equal to the following integral over $u = \varepsilon_k/\Delta_0$:

$$\tilde{F}(x; \tilde{q}, \tilde{\omega}) = \int_{-\infty}^{+\infty} \frac{du}{V} \frac{V_-^2 - V^2 - \tilde{\omega}^2}{[(V_- + V)^2 - (\tilde{\omega} + i\delta)^2][(V_- - V)^2 - (\tilde{\omega} + i\delta)^2]} \tag{A6}$$

Here we have introduced

$$V^2 \equiv u^2 + \rho_x^2; \qquad V_-^2 \equiv (u - \tilde{q}x)^2 + \rho_x^2 \tag{A7}$$

The real and imaginary parts of Eq. (A6) become equal to

$$\operatorname{Re} F(x;\tilde{q},\tilde{\omega}) = P\int_{-\infty}^{+\infty} \frac{du}{(u^2+\rho_x^2)^{1/2}} \frac{[(\tilde{q}x)^2-\tilde{\omega}^2-2\tilde{q}xu]}{4[(\tilde{q}x)^2-\tilde{\omega}^2](u-u_x^+)(u-u_x^-)} \tag{A8}$$

$$\begin{aligned}\operatorname{Im} \tilde{F}(x;\tilde{q},\tilde{\omega}) = -\pi \int_{-\infty}^{+\infty} & \frac{du}{(u^2+\rho_x^2)^{1/2}} [(\tilde{q}x)^2-\tilde{\omega}^2-2\tilde{q}xu] \\ & \times \operatorname{sgn}\{\tilde{\omega}^2-[u^2+(u-\tilde{q}x)^2+2\rho_x^2]\} \\ & \times \delta\{4[(\tilde{q}x)^2-\tilde{\omega}^2](u-u_x^+)(u-u_x^-)\}\end{aligned} \tag{A9}$$

Here $u_x^+$ and $u_x^-$ are the roots of the denominator expression in Eq. (A6), which is a second-order polynomial in $u$:

$$u_x^{\pm} = \frac{1}{2}\left[\tilde{q}x \pm \left(\tilde{\omega}^2 + \frac{4\tilde{\omega}^2\rho_x^2}{\tilde{q}^2x^2-\tilde{\omega}^2}\right)^{1/2}\right] \tag{A10}$$

For simplicity we specialize now to $\rho_x^2 = 1-x^2$, that is, we neglect the correction terms of order $\mu$ in the expressions (A2) and (A3) for the energy gap. It is not difficult to generalize the following steps to include the full energy gap expression in Eq. (A3). It is important to differentiate between the two cases where $\tilde{\omega} > \tilde{q}$ and where $\tilde{\omega} < \tilde{q}$. The roots given in Eq. (A10) become real only if one of the following two conditions is satisfied:

$$1-(\tilde{\omega}^2-\tilde{q}^2)/(4-\tilde{q}^2) < x^2 \le 1 \qquad (\tilde{\omega} > \tilde{q}) \tag{A11}$$

$$(\tilde{\omega}/\tilde{q})^2 < x^2 \le 1 \qquad (\tilde{\omega} < \tilde{q}) \tag{A12}$$

If either one of the inequalities (A11) or (A12) is satisfied, the evaluation of the integrals over $u$ in Eqs. (A8) and (A9) leads to the expressions

$$\begin{aligned}\operatorname{Re} \tilde{F}(x;\tilde{q},\tilde{\omega}) = & \frac{1}{4}\frac{1}{\tilde{\omega}^2-\tilde{q}^2x^2} \\ & \times\left[\tilde{\omega}\left(1+\frac{4\rho_x^2}{\tilde{q}^2x^2-\tilde{\omega}^2}\right)^{-1/2}(S_x^+-S_x^-)+\tilde{q}x(S_x^++S_x^-)\right]\end{aligned} \tag{A13}$$

where

$$S_x^{\pm} = [(u_x^{\pm})^2+\rho_x^2]^{-1/2} \ln\left|\frac{u_x^{\pm}-[(u_x^{\pm})^2+\rho_x^2]^{1/2}}{u_x^{\pm}+[(u_x^{\pm})^2+\rho_x^2]^{1/2}}\right| \tag{A14}$$

and

$$\operatorname{Im}\tilde{F}(x;\tilde{q},\tilde{\omega})=\frac{\pi}{4}\frac{1}{|\tilde{\omega}^2-\tilde{q}^2x^2|}\left\{\tilde{\omega}\left(1+\frac{4\rho_x^2}{\tilde{q}^2x^2-\tilde{\omega}^2}\right)^{-1/2}\right.$$
$$\times\left[\frac{\operatorname{sgn}_x^+}{[(u_x^+)^2+\rho_x^2]^{1/2}}+\frac{\operatorname{sgn}_x^-}{[(u_x^-)^2+\rho_x^2]^{1/2}}\right]$$
$$\left.+\tilde{q}x\left[\frac{\operatorname{sgn}_x^+}{[(u_x^+)^2+\rho_x^2]^{1/2}}-\frac{\operatorname{sgn}_x^-}{[(u_x^-)^2+\rho_x^2]^{1/2}}\right]\right\} \tag{A15}$$

where

$$\operatorname{sgn}_x^{\pm}=\operatorname{sgn}\{\tilde{\omega}^2-[(u_x^{\pm})^2-(u_x^{\pm}-\tilde{q}x)^2+2\rho_x^2]\} \tag{A16}$$

It turns out that Im $\tilde{F}$ given by Eqs. (A15) and (A16) vanishes exactly if the condition in Eq. (A12) is satisfied. However, if the condition in Eq (A11) is met, Im $\tilde{F}$ becomes finite. Analytical evaluation of Eq. (A15) leads then to the values of the $x$ integrals given by Eqs. (B11)–(B13) for the limit $\tilde{q}\to 0$ ($\tilde{\omega}>0$).

Finally, we quote the results where the conditions (A11) and (A12) are not satisfied. Then the roots of the denominator polynomial in Eq. (A6), $u_x^{\pm}$, become complex conjugate, i.e.,

$$u_x^{\pm}=\frac{1}{2}\left[\tilde{q}x\pm i|\tilde{\omega}|\left(\left|1+\frac{4\rho_x^2}{\tilde{q}^2x^2-\tilde{\omega}^2}\right|\right)^{1/2}\right] \tag{A17}$$

Then Im $\tilde{F}\equiv 0$, and Re $\tilde{F}$ becomes equal to

$$\operatorname{Re}\tilde{F}(x;\tilde{q},\tilde{\omega})=\frac{1}{2}\frac{1}{\tilde{\omega}^2-\tilde{q}^2x^2}\left\{\tilde{\omega}\left(\left|1+\frac{4\rho_x^2}{\tilde{q}^2x^2-\tilde{\omega}^2}\right|\right)^{-1/2}\operatorname{Im}S_x^+ +\tilde{q}x\operatorname{Re}S_x^+\right\} \tag{A18}$$

where

$$S_x^+=[(u_x^+)^2+\rho_x^2]^{-1/2}\left(\ln\left\{\frac{u_x^+}{\rho_x}-\left[\left(\frac{u_x^+}{\rho_x}\right)^2+1\right]^{1/2}\right\}\right.$$
$$\left.-\ln\left\{\frac{u_x^+}{\rho_x}+\left[\left(\frac{u_x^+}{\rho_x}\right)^2+1\right]^{1/2}\right\}\right) \tag{A19}$$

for

$$0\le x^2<1-\frac{\tilde{\omega}^2-\tilde{q}^2}{4-\tilde{q}^2}\qquad(\tilde{\omega}>\tilde{q}) \tag{A20}$$

$$0\le x^2<(\tilde{\omega}/\tilde{q})^2\qquad(\tilde{\omega}<\tilde{q}) \tag{A21}$$

The expressions for Re $F$ given by Eqs. (A13) and Eq. (A18), respectively, have been inserted into the $x$ integrals for $a_x$, $a_y$, and $b$ given by Eqs. (20)–(22) and then these integrals have been carried out numerically.

## APPENDIX B. ANGLE AVERAGES OF $F$

In calculating $\chi_{\text{spin}}$, $\chi_{\text{orb}}$, and $g_n$ [see Eqs. (27)–(29)] we need integrals of $x^{2m}\tilde{F}(x;\tilde{q},\tilde{\omega})$ over $x=\cos\theta=\hat{k}_y$ from $x=-1$ to $x=+1$. These integrals have been carried out analytically in the limit $\tilde{q}\to 0$ (but $\tilde{\omega}>0$). The dominating contributions to the real parts of these integrals arise from the region of $x$ where $0\le x^2<1-(\tilde{\omega}/2)^2$ [see Eq. (A20)], where Re $\tilde{F}$ is given by Eq. (A18). In the limit $\tilde{q}\to 0$ this yields the following integrals:

$$I_1^{(m)}=\frac{1}{\tilde{\omega}}\int_0^a dx\,\frac{x^{2m}}{(a^2-x^2)^{1/2}}\,\mathrm{Im}\ln\frac{i(a^2-x^2)^{1/2}-(\tilde{\omega}/2)}{i(a^2-x^2)^{1/2}+(\tilde{\omega}/2)} \tag{B1}$$

where $a^2\equiv 1-(\tilde{\omega}/2)^2$. The results of these integrals for $m=0$, 1, and 2 are given in terms of the following functions of $\tilde{\omega}/2a$:

$$\begin{aligned} f&\equiv \ln\{(\tilde{\omega}/2a)+[1+(\tilde{\omega}/2a)^2]^{1/2}\}\\ g&\equiv \ln\frac{[1+(\tilde{\omega}/2a)^2]^{1/2}+1}{[1+(\tilde{\omega}/2a)^2]^{1/2}-1}\\ h&\equiv \sum_{k=0}^{\infty}\frac{2-2^{2k}}{(2k+1)!}B_{2k}f^{2k+1}\qquad(\tilde{\omega}<2)\end{aligned} \tag{B2}$$

where the $B_{2k}$ are Bernoulli numbers. Then we have

$$I_1^{(0)}=\tilde{\omega}^{-1}fg+2\tilde{\omega}^{-1}h \tag{B3}$$

$$I_1^{(1)}=\tfrac{1}{2}\tilde{\omega}^{-1}a^2\{f+(\tilde{\omega}/2a)[1+(\tilde{\omega}/2a)^2]^{1/2}\}g+\tilde{\omega}^{-1}a^2h-\tfrac{1}{2}a \tag{B4}$$

$$\begin{aligned} I_1^{(2)}=\tilde{\omega}^{-1}a^4\{&\tfrac{3}{8}f+[\tfrac{5}{8}+\tfrac{1}{4}(\tilde{\omega}/2a)^2](\tilde{\omega}/2a)[1+(\tilde{\omega}/2a)^2]^{1/2}\}g\\ &+\tfrac{3}{4}\tilde{\omega}^{-1}a^4h-(17/24)a^3-\tfrac{1}{16}a\tilde{\omega}^2\end{aligned} \tag{B5}$$

The remaining contributions to the $x$ integrals over $x_{2m}\,\mathrm{Re}\,\tilde{F}$ are determined by Eq. (A13). In the limit $\tilde{q}\to 0$ ($\tilde{\omega}>0$) we obtain with the help of Eqs. (A10), (A11), and (A14) the contributions

$$I_2^{(m)}=-\frac{1}{\tilde{\omega}}\int_a^1 dx\,\frac{x^{2m}}{(x^2-a^2)^{1/2}}\ln\frac{(\tilde{\omega}/2)+(x^2-a^2)^{1/2}}{(\tilde{\omega}/2)-(x^2-a^2)^{1/2}} \tag{B6}$$

The results for $m=0$, 1, and 2 are found to be

$$I_2^{(m)}=\frac{1}{2}\sum_{n=0}^{\infty}(-1)^n\binom{m-\frac{1}{2}}{n}\left(\frac{\tilde{\omega}}{2}\right)^{2n}L_n\qquad(\tilde{\omega}<2) \tag{B7}$$

where

$$L_n = \int_0^1 dt\,(1-t^2)^n \ln\frac{1-t}{1+t} \tag{B8}$$

For $L_n$ we find the following recursion relation:

$$L_{n+1} = \frac{2n+2}{2n+3} L_n + \frac{1}{(n+1)(2n+3)} \qquad (n = 0, 1, 2, \ldots) \tag{B9}$$

It is $L_0 = -2 \ln 2$.

For the low-frequency modes ($\tilde{\omega} \sim \sqrt{\mu} \ll 1$) the contributions to $\chi_{\text{spin}}$, $\chi_{\text{orb}}$, and $g_n$ arising from the terms $I_2^{(m)}$ can be neglected in comparison to the contributions due to the terms $I_1^{(m)}$. However, for the high-frequency modes ($\tilde{\omega} \sim 1$) the $I_2^{(m)}$ are of the same order of magnitude as the $I_1^{(m)}$.

The imaginary part of $\tilde{F}$ is given by Eq. (A15). In the limit $\tilde{q} \to 0$ ($\tilde{\omega} > 0$) it is different from zero only for values of $x$ satisfying the inequality $a^2 < x^2 \leq 1$ [see Eq. (A11)]. With the help of Eqs. (A10) and (A16) we find from Eq. (A15)

$$\operatorname{Im} \tilde{F}(x; 0, \tilde{\omega}) = \frac{\pi}{2\tilde{\omega}} \frac{1}{(x^2 - a^2)^{1/2}} \tag{B10}$$

This yields

$$2\int_a^1 dx\, \operatorname{Im} \tilde{F} = \frac{\pi}{2\tilde{\omega}} \ln\frac{1+(\tilde{\omega}/2)}{1-(\tilde{\omega}/2)} \tag{B11}$$

$$2\int_a^1 dx\, x^2 \operatorname{Im} \tilde{F} = \frac{\pi}{4\tilde{\omega}}\left[\tilde{\omega} + \left(1 - \frac{\tilde{\omega}^2}{4}\right) \ln\frac{1+(\tilde{\omega}/2)}{1-(\tilde{\omega}/2)}\right] \tag{B12}$$

$$2\int_a^1 dx\, x^4 \operatorname{Im} \tilde{F} = \frac{\pi}{8} + \frac{3}{4}\left(1 - \frac{\tilde{\omega}^2}{4}\right) 2\int_a^1 dx\, x^2 \operatorname{Im} \tilde{F} \tag{B13}$$

With the help of Eqs. (B11)–(B13) we obtain for $\tilde{\omega} \ll 1$ the results for $\operatorname{Im} \chi_{\text{spin}}$, $\operatorname{Im} \chi_{\text{orb}}$, and $\operatorname{Im} g_n$ as given in Eq. (30).

## APPENDIX C. CALCULATION OF THE SUSCEPTIBILITY $\chi_{GG}$

Carrying out the frequency sums in the expression for $\chi_{GG}$ in Eq. (9), we find after analytical continuation of $i\omega_m$ to $(\omega + i\delta)$

$$\chi_{GG}(\mathbf{q}, \omega) = N(0) \int \frac{d\Omega}{4\pi} \int_{-\infty}^{+\infty} d\varepsilon_k \frac{1}{[(\omega+i\delta)^2 - (E_k + E_{k+q})^2][(\omega+i\delta)^2 - (E_{k+q} - E_k)^2]}$$

$$\times \left\{ \frac{1}{E_k} \tanh\frac{E_k}{2T} [(E_{k+q}^2 + E_k^2 - \omega^2)(E_k^2 - \varepsilon_{k+q}\varepsilon_k) - 2E_k^2(E_{k+q}^2 - \varepsilon_{k+q}\varepsilon_k)] \right.$$

$$+\frac{1}{E_{k+q}}\tanh\frac{E_{k+q}}{2T}[(E_{k+q}^2+E_k^2-\omega^2)(E_{k+q}^2-\varepsilon_{k+q}\varepsilon_k) \\ -2E_{k+q}^2(E_k^2-\varepsilon_{k+q}\varepsilon_k)]\Big\} \quad \text{(C1)}$$

In this paper we specialize Eq. (C1) to $T\to 0$ and to $\mathbf{q}\|\boldsymbol{l}$. We make use of the fact that the denominator expression in the integrand of Eq. (C1) is identical to that of the function $F$, Eq. (23). This denominator is a second-order polynomial in the reduced energy variable $u\equiv\varepsilon_k/\Delta_0$. The upper and lower limits of the $u$ integral are set equal to $U$ and $-U$, and at the end of the calculation the limit $U\to\infty$ is taken. Then we can rewrite $\chi_{GG}$ as follows:

$$\chi_{GG}(\mathbf{q},\omega)=\lim_{U\to\infty}\frac{1}{2}N(0)\int_{-1}^{+1}dx\left(\int_{-U}^{+U}du+\int_{-U+\tilde{q}x}^{+U+\tilde{q}x}du\right)\frac{1}{(u^2+\rho_x^2)^{1/2}} \\ \times\left(\frac{\tilde{q}xu}{(\tilde{q}x)^2-(\tilde{\omega}+i\delta)^2}+\frac{\tilde{\omega}^2+(\tilde{q}x)^2}{[(\tilde{\omega}-i\delta)^2-(\tilde{q}x)^2]}\rho_x^2\right. \\ \times[(\tilde{q}x)^2-\tilde{\omega}^2-2\tilde{q}xu] \\ \times\{4[(\tilde{q}x)^2-(\tilde{\omega}+i\delta)^2][u^2-\tilde{q}xu] \\ \left.+[(\tilde{q}x)^2-(\tilde{\omega}+i\delta)^2]^2-4\rho_x^2(\tilde{\omega}+i\delta)^2\}^{-1}\right) \quad \text{(C2)}$$

Here $\rho_x^2$ is the reduced energy gap squared [see Eq. (A3)], and $\tilde{q}$ and $\tilde{\omega}$ are the reduced wave number and frequency variables [see Eq. (A5)]. The first term on line 2 in Eq. (C2) yields the Lindhard function and the second term on line yields, apart from a factor, the function $\tilde{F}$ given by Eq. (A6). In this way we obtain for the real part of $\chi_{GG}$

$$\operatorname{Re}\chi_{GG}(\mathbf{q},\omega)=N(0)\left[2-\frac{\omega}{v_Fq}\ln\left|\frac{\omega+v_Fq}{\omega-v_Fq}\right|\right] \\ +N(0)P\int_{-1}^{+1}dx\,\frac{\tilde{\omega}^2+(\tilde{q}x)^2}{\tilde{\omega}^2-(\tilde{q}x)^2}\rho_x^2\operatorname{Re}\tilde{F}(x;\tilde{q},\tilde{\omega}) \quad \text{(C3)}$$

The imaginary part of $\chi_{GG}$ consists of the well-known imaginary part of the Lindhard function plus a rather complicated expression due to $\tilde{F}$ which we shall not write down.

## ACKNOWLEDGMENTS

We are grateful to D. Einzel for assistance in the early stage of this work. We also profited from discussions with D. Fay, P. Kumar, A. J. Leggett, K. Maki, S. Takagi, and P. Wölfle.

## REFERENCES


1. L. Tewordt, D. Fay, P. Dörre, and D. Einzel, *J. Low Temp. Phys.* **21**, 645 (1975) (hereafter referred to as TFDE).
2. L. Tewordt and D. Einzel, *Phys. Lett.* **56A**, 97 (1976).
3. A. J. Leggett and S. Takagi, *Phys. Rev. Lett.* **36**, 1379 (1976).
4. L. Tewordt and D. Einzel, *Bulletin Frühjahrstagung Deutsche Physikalische Gesellschaft, Freudenstadt* (April 1976).
5. P. Wölfle, *Phys. Rev. Lett.* **37**, 1279 (1976); and to be published.
6. A. J. Leggett, *Rev. Mod. Phys.* **47**, 331 (1975).
7. M. C. Cross, *J. Low Temp. Phys.* **26**, 165 (1977).
8. R. Combescot, *Phys. Rev. Lett.* **35**, 1646 (1975).
9. B. R. Patton, in *Proc. of the 14th Int. Conf. on Low Temp. Phys., Otaniemi, Finland, 1975*, M. Krusius and M. Vuorio, eds. (North-Holland, Amsterdam, 1975), Vol. 1, p. 17.
10. P. W. Anderson, *Phys. Rev.* **112**, 1900 (1958).
11. N. N. Bogoliubov, V. V. Tolmachev, and D. N. Shirkov, *New Method in the Theory of Superconductivity* (English transl.: Consultants Bureau, New York, 1959).
12. J. C. Wheatley, *Rev. Mod. Phys.* **47**. 415 (1975).